

PHOTOELECTRIC INSTRUMENTS AND THE MEASUREMENT OF AEROSOL MICROSTRUCTURE

L.N. Pavlova

*Institute of Experimental Meteorology, Obninsk
Scientific-Production Company "Taifun", Obninsk
Goskomgidromet SSSR, Obninsk
Received September 5, 1989*

In this paper the effect of particle index of refraction on the results obtained for the distribution function of particles over size using a photoelectric instrument to record the light scattering to the side is studied. The instrument operates in tandem with an eight-channel pulse-height analyzer; the minimum detectable signal corresponds to an equivalent latex radius of $r = 0.1 \mu\text{m}$.

The photoelectric method of determining the size and concentration of particles involves illuminating them by a beam of light, counting the light pulses from each particle over a certain scattering angle range in pulse-counting mode, and then analyzing the amplitude values for the particles. If the relationship between pulse height and particle size is known, the latter can be determined for the particles passing through the operating volume of the instrument. However, there are several difficulties which arise in interpreting the results of measurements obtained by this method. The effect of various factors on the accuracy with which the microstructural characteristics of a disperse medium can be determined have been discussed by several researchers (see the papers by Belyaev, et al.¹ and Quenzel⁶).

One of the reasons for the difficulty in interpreting the results of the measurements is the fact that the instrument calibration (i.e., the relationship between amplitude and particle radius) is generally carried out using calibrated latex spheres with Index of refraction $m = 1.49$ or $1.58^{2,6}$ or droplets of transformer oil ($m = 1.50$),¹ while we are frequently studying particles with unknown m . Moreover, the medium may contain a mixture of particles with different chemical compositions (for example, the atmosphere).

Belyaev, et al.,¹ Kozlov, et al.,³ and Quenzel⁶ have shown that it is impossible to obtain high instrumental resolution in this case, and the errors in determining the diameters of the individual particles may run as high as 350%, especially when laser spectrometers are used. However, when photoelectric instruments are used to study the atmospheric aerosol, the microstructural characteristics are determined in terms of a so-called latex equivalent.

In this paper, we use a numerical simulation to study the distortion of the particle size distribution functions $f(r)$ for various substances determined by a photoelectric instrument calibrated using latex spheres with $m = 1.49$. The calculations were carried out for the most commonly used instrument design, in which

the light scattered by the particles is recorded from the side ($\Theta = 90^\circ \pm 10^\circ$). We assume (1) that the medium consists of homogeneous spherical particles, and (2) that the particles are illuminated by a beam of laser light with wavelength $\lambda = 0.63 \mu\text{m}$ or by a beam of "white light" (angle of divergence $2\gamma = 10^\circ$).

The problem was solved in the following fashion: First of all, the directed light scattering coefficients $F(\Theta, r, m)$ were calculated for particles of various chemical composition with radii $r = 0.01$ (0.01) $5.0 \mu\text{m}$ under illumination by light with $\lambda = 0.63 \mu\text{m}$ and by "white light" using Mie theory. The geometry of the measurement process was taken into account using the formulas presented by Hodkinson and Greenfield.⁵

The "white-light" results were obtained by integrating over λ from $0.38 \mu\text{m}$ to $0.83 \mu\text{m}$ (with $\Delta\lambda = 0.05 \mu\text{m}$) without taking into account the spectral characteristics of the source and detector into account, since this provides the best smoothing of the oscillations in the scattered light (relative to the case for monochromatic illumination).

The calculations were carried out for (a) latex spheres, $m = 1.49$; (b) the soluble fraction of the atmospheric aerosol,⁴ $m = 1.53 - 0.006i$; (c) water, $m = 1.33$; (d) dust⁴ $m = 1.53 - 0.008i$; and, (e) soot⁴ $m = 1.75 - 0.43i$.

The results of the calculations of $F(\Theta, r, m)$ for laser light with $\lambda = 0.63 \mu\text{m}$ are shown in Fig. 1 (the curve for dust is virtually identical to curve 2. and is not shown). Despite the fact that the intensity of the scattered light is averaged over the solid angle of the detector, oscillations are observed in the values of $F(\Theta, r, m)$ for particles with weak absorption or no absorption and $r > 0.7 \mu\text{m}$, as previously noted by Quenzel.⁶ There are no oscillations in the case of soot because of the substantial light absorption. The oscillations are essentially smoothed out in the "white-light" case, although there is still some difference between the curves for various m (these curves have been

presented many times in the literature — see Belyaev, et al.,¹ for example). We shall discuss the operation of this instrument in combination with an 8-channel pulse-height analyzer.

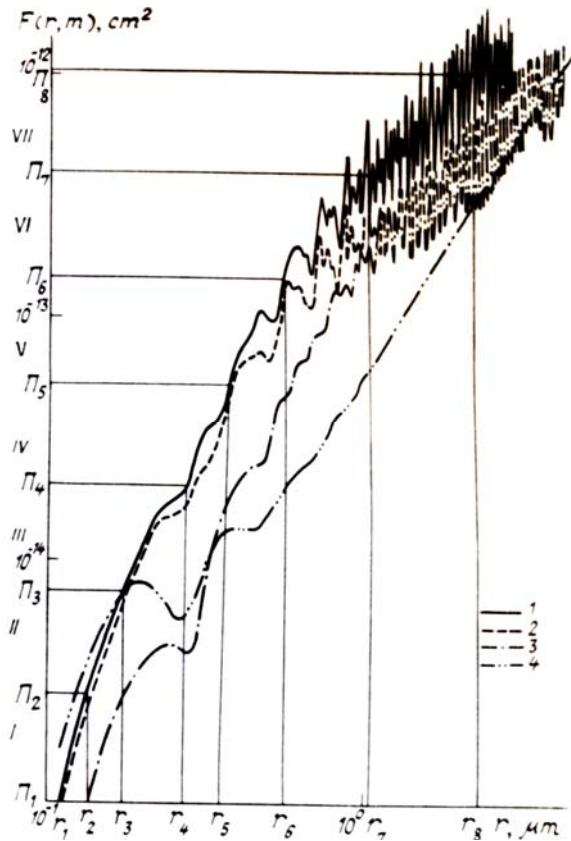


FIG. 1. Directional scattering coefficient at $\Theta = 90^\circ \pm 5^\circ$ as a function of particle radius at various indices of refraction: 1) $m = 1.49$, 2) $m = 1.53 - 0.006i$; 3) $m = 1.33$, 4) $m = 1.75 - 0.43i$. The roman numerals I–VII indicate the ranges of values for $F(r, m)$ corresponding to channels 1–7 of the pulse-height analyzer; $r_1 - r_8$ indicate the threshold values for latex-sphere particle radii for each channel.

The range of values occupied by $\log F(\Theta, r, m)$ for $m = 1.49$ [(which corresponds to three orders of

magnitude of variation in $F(\Theta, r, m)$] was divided into seven equal intervals as shown in Fig. 1, and the threshold values of $F(r)$ for the 8-channel pulse-height analyzer ($\Pi_1 - \Pi_8$) were determined. The threshold value for analyzer channel 1 was chosen to be equal to $F(r)$ for latex particles with $r = 0.1 \mu\text{m}$. Figure 1 clearly indicates that each interval of values $\Delta F_k(r)$ corresponding to analyzer channel k corresponds to different intervals in radius Δr_k for particles with various m .

The operation of the 8-channel pulse-height analyzer was modelled in the following way. It was assumed that the particles in the medium have a log-normal distribution over size:

$$f(r) = \frac{N_0}{\sqrt{2\pi} \ln \sigma \cdot r} \exp \left[-\frac{1}{2} \left\{ \frac{\ln(r_m/r)}{\ln \sigma} \right\}^2 \right], \quad (1)$$

where N_0 is the total number of particles per unit volume, r_m is the median (or geometric mean) radius, and σ is a parameter characterizing the width of the distribution.

The values $r_m = 0.03, 0.15, 0.25, 0.5,$ and $1.0 \mu\text{m}$, and $\sigma = 2$ and 3 . For each fixed radius value from $r = 0.01 \mu\text{m}$ to $r = 20r_m$, we determined $F(r, m)$ and the number of particles $\Delta n = f(r) \cdot \Delta(r)$ in the medium with radii from r to $r + \Delta r$ with $\Delta r = 0.01 \mu\text{m}$. The sum of the values of Δn for those particles with $F(r, m) < \Pi_1$ determines the number of pulses not recorded by the instrument. Pulses for which $\Pi_k \leq F(r, m) < \Pi_{k+1}$ are recorded in the k th channel of the pulse-height analyzer. For $F(r, m) \geq \Pi_8$ all pulses are recorded in channel 8.

The results of the calculation for the case where the particles are illuminated using laser light with $\lambda = 0.63 \mu\text{m}$ for $\sigma = 2$ and 3 are given in Tables I and II, respectively. The fraction of the total number of pulses $n_k = N_k/N_0$ falling within each channel was then determined for channels 1–8. The last row of Table I contains the values for $\sum_1^8 n_k$.

TABLE I.

Fraction of impulses $\Delta n_k/N_0$ (%) recorded in each channel of the pulse-height analyzer for various r_m at $\delta = 2$.

| Channel number | $r_m, \mu\text{m}$ | $r_m = 0.03 \mu\text{m}$ | | | | $r_m = 0.15 \mu\text{m}$ | | | | $r_m = 0.25 \mu\text{m}$ | | | | $r_m = 0.5 \mu\text{m}$ | | | |
|----------------|--------------------|--------------------------|------------------|-------|------|--------------------------|------------------|-------|------|--------------------------|------------------|-------|------|-------------------------|------------------|-------|------|
| | | Latex | Soluble fraction | Water | Soot | Latex | Soluble fraction | Water | Soot | Latex | Soluble fraction | Water | Soot | Latex | Soluble fraction | Water | Soot |
| 1 | 0.10 | 2.8 | 2.2 | 1.5 | 3.1 | 14.1 | 9.6 | 13.0 | 9.7 | 7.7 | 5.0 | 8.5 | 4.6 | 1.4 | 0.9 | 2.0 | 0.7 |
| 2 | 0.13 | 1.1 | 1.7 | 1.1 | 2.0 | 12.3 | 16.8 | 34.2 | 13.6 | 8.6 | 11.4 | 35.9 | 8.2 | 2.3 | 2.8 | 17.1 | 1.7 |
| 3 | 0.16 | 0.78 | 0.61 | 0.03 | 1.5 | 25.9 | 15.5 | 5.4 | 50.6 | 26.6 | 14.2 | 8.9 | 61.9 | 12.0 | 5.4 | 7.3 | 41.6 |
| 4 | 0.26 | 0.08 | 0.25 | 0.02 | 0.0 | 10.7 | 20.3 | 8.1 | 4.7 | 16.8 | 27.6 | 17.4 | 14.6 | 13.0 | 18.2 | 21.2 | 30.2 |
| 5 | 0.35 | 0.02 | 0.02 | 0.0 | 0 | 8.1 | 8.8 | 3.3 | 0.73 | 18.5 | 19.4 | 10.7 | 4.0 | 24.3 | 24.6 | 23.0 | 17.5 |
| 6 | 0.55 | 0 | 0 | 0 | 0 | 3.1 | 3.4 | 0.9 | 0.07 | 11.8 | 13.2 | 5.0 | 0.7 | 33.3 | 38.7 | 21.8 | 6.1 |
| 7 | 1.09 | 0 | 0 | 0 | 0 | 0.2 | 0.1 | 0.0 | 0 | 1.6 | 1.0 | 0.5 | 0.1 | 10.7 | 7.7 | 5.5 | 1.3 |
| 8 | 2.21 | 0 | 0 | 0 | 0 | 0 | 0 | 0 | 0 | 0.1 | 0 | 0 | 0 | 2.1 | 0.7 | 0.3 | 0.2 |
| $\Sigma, \%$ | — | 4.78 | 4.78 | 2.65 | 6.6 | 74.4 | 74.5 | 64.9 | 79.3 | 91.7 | 91.8 | 86.9 | 94.1 | 99.1 | 99.0 | 98.2 | 99.3 |

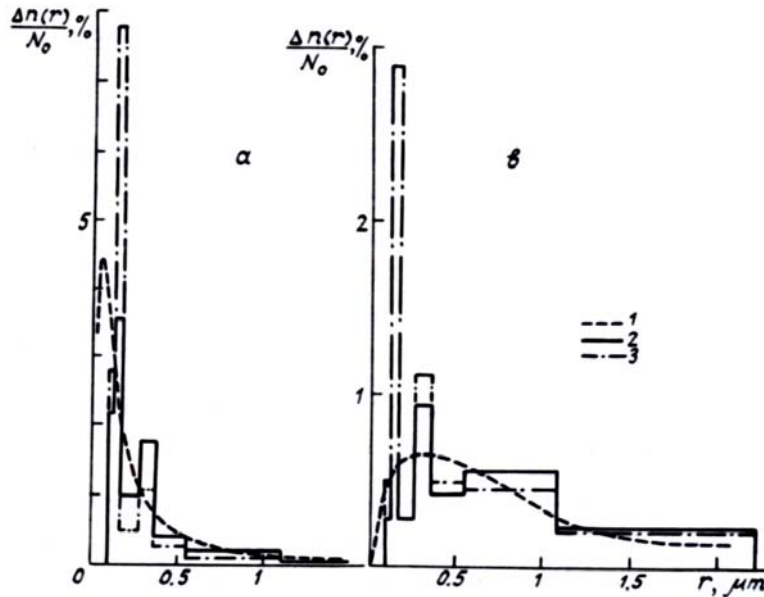


FIG. 2. Initial particle size distribution (1) and particle size distribution determined by the instrument (2 - soluble fraction, 3 - water) when particles are illuminated by light with $\lambda = 0.63 \mu\text{m}$, $r_m = 0.15 \mu\text{m}$, $\sigma = 3$ (a); $r_m = 1.0 \mu\text{m}$, $\sigma = 3$ (b).

TABLE II.

Fraction of impulses $\Delta n_k/N_0$ (%) recorded in each channel of the pulse-height analyzer for various r_m at $\delta = 3$.

| Channel number | $r_k, \mu\text{m}$ | $\bar{r}_k, \mu\text{m}$ | $r_m = 0.15 \mu\text{m}$ | | | | $r_m = 0.25 \mu\text{m}$ | | | | $r_m = 0.5 \mu\text{m}$ | | | |
|----------------|--------------------|--------------------------|--------------------------|------------------|-------|------|--------------------------|------------------|-------|------|-------------------------|------------------|-------|------|
| | | | Latex | Soluble fraction | Water | Soot | Latex | Soluble fraction | Water | Soot | Latex | Soluble fraction | Water | Soot |
| 1 | 0.10 | 0.115 | 9.5 | 6.6 | 8.3 | 7.0 | 7.5 | 5.1 | 7.0 | 5.2 | 3.8 | 2.5 | 3.9 | 2.4 |
| 2 | 0.13 | 0.145 | 7.8 | 10.7 | 23.3 | 8.9 | 6.8 | 9.2 | 23.5 | 7.3 | 4.0 | 5.3 | 17.4 | 3.9 |
| 3 | 0.16 | 0.21 | 17.4 | 10.0 | 4.7 | 38.2 | 17.5 | 9.7 | 5.7 | 42.0 | 12.7 | 6.5 | 5.3 | 34.9 |
| 4 | 0.26 | 0.305 | 9.0 | 15.6 | 9.4 | 9.2 | 10.8 | 17.7 | 12.8 | 14.7 | 9.8 | 14.9 | 13.9 | 19.8 |
| 5 | 0.35 | 0.45 | 10.0 | 10.5 | 6.8 | 4.1 | 14.0 | 14.5 | 11.0 | 8.3 | 15.7 | 16.0 | 15.0 | 15.3 |
| 6 | 0.55 | 0.82 | 8.9 | 10.2 | 5.3 | 1.6 | 15.6 | 18.4 | 10.7 | 4.0 | 24.4 | 29.4 | 20.0 | 9.7 |
| 7 | 1.09 | 1.65 | 2.7 | 2.0 | 1.4 | 0.4 | 6.1 | 5.2 | 4.3 | 1.6 | 13.8 | 12.9 | 11.7 | 5.1 |
| 8 | 2.21 | 2.21 | 0.5 | 0.1 | 0.0 | 0.0 | 2.3 | 1.1 | 0.4 | 0.4 | 9.0 | 5.6 | 3.3 | 3.2 |
| $\Sigma, \%$ | — | — | 65.8 | 65.7 | 59.2 | 69.4 | 80.6 | 80.9 | 75.4 | 83.5 | 93.2 | 93.1 | 90.5 | 94.3 |

The table indicates that when the distribution functions for the particles over size are identical, the pulse-height-channel distributions of the pulses are different for different materials. In order to go from these data to the size distribution, we must determine the particle-radius boundaries of each channel r_k .

Assume that these values were determined for latex spheres with $m = 1.49$, (see Table I), and measurements for all other particles are expressed in terms of the so-called latex equivalent. Figure 2 clearly shows how the particle size distribution $\Delta n(r)$ is affected as the chemical composition of the particles varies if no correction for the variation in m is introduced (or if the values of m are unknown). The values of $\Delta n(r)/N_0$ in Fig. 2 have been transformed to intervals $\Delta r = 0.01 \mu\text{m}$. Even for the soluble fraction of the

aerosol, we see distortion of the particle size spectrum and false maxima [in spite of the fact that the $F(r, m)$ curve for them is similar to that for latex]. Figure 3 shows the particle size histograms obtained for water and the soluble fraction expressed in terms of the latex equivalent when the particles are illuminated by "white light" and the curves $F(r, m)$ are smooth. Some distortion of the size spectrum is observed for water droplets. Various moments of the particle size distribution were determined from the resulting histograms. The moments calculated using the following expressions:

$$\text{mean radius: } \bar{r}_1 = \frac{\sum_1^7 (n_k \cdot \bar{r}_k)}{\sum_1^7 N_k},$$

$$\text{root-mean-square radius: } r_{21}^2 = \frac{\sum_1^7 (N_k \cdot \bar{r}_k^2)}{\sum_1^7 N_k},$$

mean cube of the radius:

$$r_{31}^3 = \frac{\sum_1^7 (N_k \cdot \bar{r}_k^3)}{\sum_1^7 N_k},$$

volumetric density of particles:

$$V_1 = \frac{4}{3} \pi r_{31}^3 \cdot \sum_1^8 N_k \mu\text{m}^3/\text{cm}^3$$

number density of particles: $N_1 = \sum_1^8 N_k$, where \bar{r}_k is

the mean radius value for the latex spheres corresponding to the k th channel.

The data from channel 8 were not used in calculating r_1 , r_{21} , and r_{31} , since the r_8 is not known for aerosols with known $f(r)$.

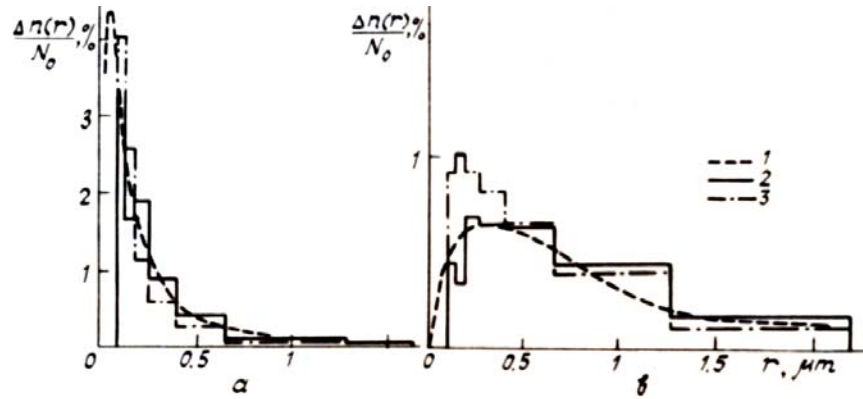


FIG. 3. Same as Fig. 2, but for "white light".

Table III gives the ratios of the calculated moments of the particle-size distribution (which we shall hereinafter call the "measured moments") to the true values for various r_m and $\sigma = 3$. These data indicate that the limited operation range of the pulse-height analyzer leads to an observed difference between the measured moments of the distribution and true moments of the distribution, even for particles with $m = 1.49$. At small $r_m = 0.03$, this difference is due to the fact that most of the small particles with $r < 0.1 \mu\text{m}$ are not recorded by the instrument ($N_1/N_0 \approx 14\%$) and this means that the mean particle radii are severely overestimated. However, the volumetric density of particles for this case is approximately equal to the true density: $V_1/V \approx 1.2$. Despite the that the modal radius r_{mode}

is within the range of radii covered by the instrument, if even a small fraction of the particles have $r > r_8$ (and are thus not taken into account in the mean-radius calculation) leads to underestimation of \bar{r}_1 , r_{21} , and r_{31} , and thus to underestimation of V_1 . The difference between the measured moments of the distribution and the corresponding moments for latex spheres is due to the difference in index of refraction in the case of the soluble aerosol fraction (and even more significantly in the case of the water droplets). The pulse-height analyzer discussed here provides the most precise determination of the mean radii for the soluble aerosol fraction and for water when $r_m = 0.15\text{--}0.25 \mu\text{m}$ ($\sigma = 3$). For larger r_m and wider particle size distributions, we must extend the operating range of the pulse-height analyzer.

Table III

Ratio of the measured moments $f(r)$ to true values "white" light being used

| | Particles with $m=1.49$ | | | | | Soluble fraction | | | | | Water | | | | |
|------------------|-------------------------|-------|-------|------|------|------------------|-------|-------|------|------|-------|-------|-------|------|------|
| r_m | 0.03 | 0.15 | 0.25 | 0.5 | 1.0 | 0.03 | 0.15 | 0.25 | 0.5 | 1.0 | 0.03 | 0.15 | 0.25 | 0.5 | 1.0 |
| r_{mod} | 0.009 | 0.045 | 0.075 | 0.15 | 0.3 | 0.009 | 0.045 | 0.075 | 0.15 | 0.3 | 0.009 | 0.045 | 0.075 | 0.15 | 0.3 |
| $N_1/N_0, \%$ | 14.4 | 65.8 | 80.8 | 93.1 | 98.1 | 14.4 | 65.8 | 80.8 | 93.1 | 98.1 | 9.4 | 56.3 | 73.3 | 89.3 | 96.8 |
| \bar{r}_1/r | 3.5 | 1.4 | 1.1 | 0.96 | 0.47 | 3.6 | 1.3 | 1.1 | 0.78 | 0.52 | 3.0 | 1.1 | 0.87 | 0.62 | 0.43 |
| r_{21}/r_2 | 2.6 | 1.2 | 0.95 | 0.64 | 0.40 | 2.7 | 1.2 | 0.92 | 0.62 | 0.40 | 2.1 | 0.98 | 0.77 | 0.52 | 0.34 |
| V_1/V | 1.2 | 0.93 | 0.43 | 0.13 | 0.03 | 1.3 | 0.77 | 0.40 | 0.12 | 0.03 | 0.39 | 0.40 | 0.23 | 0.08 | 0.02 |

Thus, a numerical simulation indicates that the particle size distribution determined by the instru-

ment when using a laser with $\lambda = 0.63 \mu\text{m}$ in photoelectric aerosol analyzers in which the scattered light

is detector from the side and the sizes are calibrated in terms of latex spheres. When m is known, we can convert from the latex r_k values to the values of r_k for any given substance using theoretical curves similar to those in Fig. 1. When studying aerosols whose index of refraction is unknown and whose index of refraction depends on the relative humidity of the air,⁷ false maxima may appear in the "latex-equivalent" measured $f(r)$. Because of this, it is better to use "white light" to illuminate the particles. However, it should be kept in mind that the moments of the distribution $f(r)$ may be quite different from the true moments even in this case (see Table III).

Even though these calculations were carried out for a specific type of instrument, the patterns noted above also exist to some extent in other instruments as well.

REFERENCES

1. S.P. Belyaev, N.K. Nikiforova, V.V. Smirnov, and G.I. Shchelchikov, *Optoelectronic Methods for Studying Aerosols*, Energoizdat, Moscow (1981), 230 pp.
2. V.P. Bisyarin, I.P. Bisyarina, and G.K. Tret'yakov, in: *Electromagnetic Waves in the Atmosphere and Outer Space*, Moscow, 231–242 (1986).
3. V.S. Kozlov, V.V. Pol'kin, and V.Y. Fadeev, *Izv. Akad. Nauk USSR, FAO* **18**, No. 4, 428–431 (1982).
4. *A Preliminary Cloudless Standard Atmosphere for Radiation Computation*, Radiation Commission, Boulder, CO USA. WSP-12 (1984), 58 pp.
5. J. Hodgkinson, and J. Greenfield *Appl. Opt.* **4**, No. 11, 1463–1474 (1965).
6. H. Quenzel. *Appl. Opt.* **8**, No. 1, 165–169 (1965).
7. T. Takamura, M. Tanaka, and T. Nakajima, *J. Metall. Soc. Jpn.* **62**, No. 3, 573–582 (1984).